Florida Energy Systems Consortium

University of Central Florida

Florida Opportunities for PV Manufacturing and Application

(Old Title: *PV Manufacturing Data Base and Florida Applications*)

PIs: D. Block, J Fenton, P. Fairey, W. Schoenfelds, R. Reedy

Description: The goal of this project is to establish a photovoltaic (PV) manufacturing and applications data base and to stimulate the development of a PV manufacturing industry and related applications in Florida. This project is now in its third year and consequences from both the national and the state perspective show the dominance of the Chinese industry. However, a strong market can eventually lead to manufacturing and, thus, the Florida opportunity. The key to Florida's PV goals are to have both a magnet and a demand. Florida is positioned to be a magnet because of its winning the DOE funded PV Manufacturing Consortium (PVMC) program and high demand is proposed through the application of PV power for electric vehicles. Details follow.

Budget: $81,120
Universities: UCF/FSEC

Progress Summary

The goal of this project was to establish a photovoltaic (PV) manufacturing and applications data base in order to stimulate the development of a PV manufacturing industry and PV applications in Florida. This project's data shows both the international and national PV manufacturing and application trends which are: China has emerged as the world leader, crystalline silicon remains the top world choice at 87% and California remains as the location with the largest installed capacity with Florida ranked at 8$^{th.}$
Florida imports almost all of its energy resources. Thus, the citizens of Florida pay $27 billion for electricity and $30 billion for gasoline giving a total output of $50 billion/year. Of this total, one-half leaves the state or our citizens lose an estimated $24 billion per year. These facts lead to two challenges – How can Florida reduce its energy costs and how can Florida's electricity power plants and transportation fuel be manufactured in Florida? In other words, can we design an energy future which allows Florida to keep this money and in return allow us to make the profits and increase jobs. We believe that there is a Florida future which allows for the vision described as follows.

First let's present data on jobs produced by the energy industries. Data shows that PV produces 23 jobs/MW, wind is 8 jobs/MW, nuclear is 4 jobs/MW, natural gas is 3 jobs/MW and coal is 0.5 jobs/MW. Since Florida can produce very little to no manufacturing in wind, nuclear or coal, the only possible manufacturing for Florida is PV. The key to manufacturing is to have both a magnet and a demand. How does Florida create both of these?

Starting with the magnet, Florida is positioned to be a magnet because of it winning the DOE funded PV Manufacturing Consortium (PVMC) program. Florida is teamed with SEMATECH of New York who is the prime and who won the DOE program (PVMC is a $50 million effort). For the SEMATECH program, Florida's task is crystalline silicon R&D which, as mentioned above, is the dominate cell material at 87%. In the Florida PVMC program, an existing 100,000 ft^2 semi-conductor facility has been dedicated to PVMC. However, the facility needs to be re-furbished with the installation of crystalline silicon pilot manufacturing assembly line. Once the pilot facility is established, the probability is very high for national PV manufacturing firms to become pilot facility users and then to follow with plants in a nearby location. This is the magnet.

The second need is demand. Demand is supplied by a concept that we have called a "game changer" or simply put, what can we do about gasoline prices? The answer is electric vehicles for our future. At this time, 26% of all Florida vehicles are small cars. And, the new electric motor drive cars, like the Nissan Leaf or plug-ins like the Chevy Volt, give us a whole new option to consider. How does electricity compare to gasoline in costs? Using the efficiency of a 33 mpg car, one kWh of electricity will produce 3 car miles for an equivalent electric car. Changing these numbers into cost values, a gasoline powered car cost 10.6 cents per mile to drive while the electric car costs 5.6 cents per mile. These numbers are for gasoline at $3.50 per gallon and for PV electricity at 16.8 cents per kWh. Thus, the cost to drive the PV powered electric car is less than half that of the gasoline car. This supplies the demand.

2011 Annual Report

In order to set the background for PV manufacturing in Florida and a PV demand, a data base of PV in the world and then the U.S. was established. Florida's opportunities and prospects are then evaluated.

World PV Manufacturing Statistics

The following Table 1 presents the world's PV manufacturing output (from Reference 1) for the years 2008, 2009 and 2010 (2010 is the latest available data).

Table 1 - World PV Output by Country/Region
All values are in megawatts (MW)

Worldwide Cell Data					
	2008	**2009**	**2010**	**10-09 Change**	**2010 Market Share**
China	2139	4077	10228	151%	43%
Taiwan	712	1553	3965	155%	17%
Europe	1996	2096	3127	49%	13%
Japan	1268	1503	2182	45%	9%
U.S.	401	580	1116	92%	5%
ROW	610	1506	3280	118%	14%
Total	7126	11315	23898	111%	100.0%
% C-Si	86%	83%	87%		

With world production established, let's next examine the individual companies that are the world's largest manufacturers. Although actual data is not presented, the results from Reference 1 show again the denomination of the Chinese and Taiwanese in the top spots. Only one U. S. company, First Solar is in the list and it is ranked at number 3. It is noted that the majority of the cells produced by First Solar are not made in the U. S.

U.S. PV Manufacturing Statistics

Now let's examine the U.S. manufacturers in more detail. The following Table 2 presents the top nine U.S. manufacturers for 2007, 2008, 2009 and 2010 (Reference 1).

Table 2 - U.S. Cell Production (Mega watts = MW)

		2007	2008	2009	2010	% Change
Solarworld	CA	35	33	72	251	249%
First Solar	AZ	120	147	153	222	45%
Suniva	GA	0	0	16	170	963%
Evergreen Solar	MA	16	27	105	158	50%
United Solar	MI	47	112	120	120	0%
Solyndra	CA	0	2	30	67	123%
BP Solar	MD	28	28	-	-	-
Schott Solar	NM	9	11	-	-	-
Global Solar	AZ	4	7	-	-	-
Other		10	77	84	128	-
Total		269	444	580	1116	92%

Next the PV installations in the U.S. by state for 2008, 2009, and 2010 are presented in Table 3 (Reference 2).

Table 3 – Top 10 States of PV Installations (MW)

State	2008	2009	2010	10-09 Change	2010 Market Share
CA	178.7	212.1	258.9	22%	29%
NJ	22.5	57.3	137.1	139%	16%
NV	14.9	3	61.4	1947%	7%
AR	6.4	21.1	54	156%	6%
CO	21.7	23.4	53.6	129%	6%
PA		3.4	46.8	1276%	5%
NM		1	42.8	4180%	5%
FL	0.5	35.7	35.2	-1%	4%
NC	4	7.8	30.7	294%	3%
TX		4	22.6	465%	3%
Others	38.6	34.7	135.2	290%	15%
Total	287.3	403.5	878.3	18%	100.0%

The above Tables show the international and national PV manufacturing and application trends. The data is summarized as follows:

- China has emerged as the world leader in both cell and module manufacturing with a production of 10,228 MW or 43% of the world share. The U.S. is ranked 5th with 1116 MW or 5% of the world total, a ranking that has remained the same for the past 4 years.

- Crystalline silicon remains the top world choice at 87% (up from 77% in 2009).

- There is only one U.S. PV company, First Solar, at #3 in the top 15 of the world production companies.

- In 2010, California remains as the location with the largest installed capacity at 258.9 MW or 30% of the U.S. market share. New Jersey is second at 137.1 MW. Florida ranks 8th at 35.2 MW following from 3rd in 2009.

Over the past three years, Florida has had numerous announcements of proposed PV manufacturing facilities, but no large scale plant has transpired. As reported above, applications have slightly dropped with the three FPL solar plants being put in production about two years ago. In addition, there have been publicized announcements concerning major PV projects in central and north Florida, but these announcements have not led to ground breaking and many PV experts question the economics of the proposed installations.

With these comments made, how does Florida become a player in this arena? History has shown a strong market can eventually lead to manufacturing and ,thus, the Florida opportunity.

Florida Options

Florida imports almost all of its energy resources. Thus, the citizens of Florida pay $27 billion for electricity and $30 billion for gasoline giving a total output of $50 billion/year. Of this total, one-half leaves the state or Florida consumers lose an estimated $24 billion per year. These facts lead to two challenges – How can Florida reduce its energy costs and how can Florida's electricity power plants and transportation fuel be manufactured in Florida? In other words, can we design an energy future which allows Florida to keep this money and in return allow us to make the profits and increase jobs. We believe that Florida's future can evolve which allows for this vision.

First let's talk about jobs produced by the energy industries. Data shows that PV produces 23 jobs/MW, wind is 8 jobs/MW, nuclear is 4 jobs/MW, natural gas is 3 jobs/MW and coal is 0.5 jobs/MW. Since Florida can produce very little to no manufacturing in wind, nuclear or coal, the only possible manufacturing for Florida is PV. The key to manufacturing is to have both a magnet and a demand. How does Florida create both of these?

Starting with the magnet, Florida is positioned to be a magnet because of it winning the DOE funded PV Manufacturing Consortium (PVMC) program. Florida is teamed with SEMATECH of New York who is the prime and who won the DOE program (PVMC is a $50 million effort) (see Figures 1 and 2). For the SEMATECH program, Florida's task is crystalline silicon R&D which, as mentioned above, is the dominate cell material at 87%. In the Florida PVMC program, a existing 100,000 ft2 semi-conductor facility has been dedicated to PVMC (see Figure 3). However, the facility needs to be re-furbished and to have a crystalline silicon pilot manufacturing assembly line installed. Once the pilot facility is established, the probability is very high for national PV manufacturing firms to become pilot facility users and then to follow with plants in a nearby location. This is the magnet.

Figure 1: PVMC Program

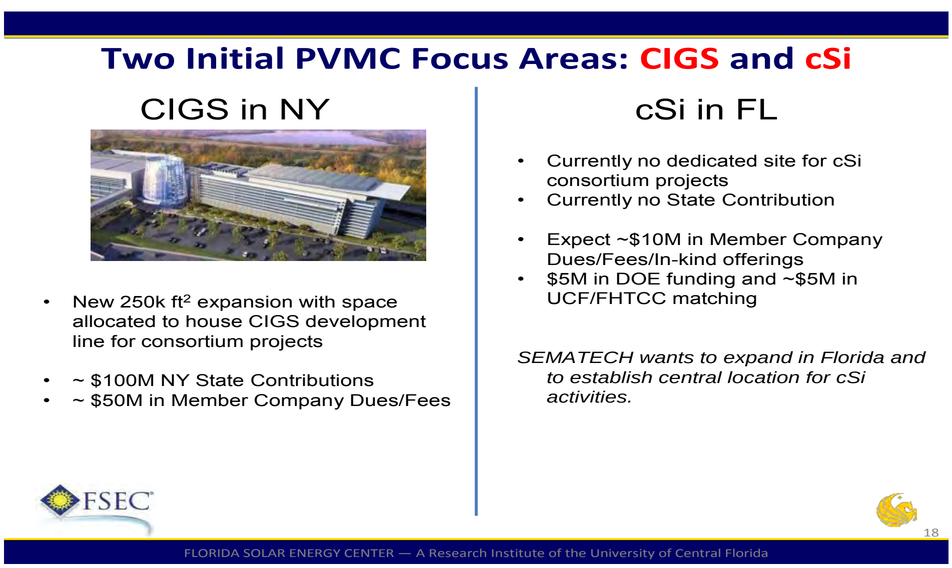

Figure 2: PVMC Focus Areas

Figure 3: UCF Facility at Palm Bay

The second need is demand. To create a demand a concept is proposed that we have called a "game changer". This concept is based on electric vehicles for our future. At this time, 26% of all Florida vehicles are small cars. And, the new electric motor drive cars, like the Nissan Leaf or plug-ins like the Chevy Volt, give us a whole new option to consider. How does electricity compare to gasoline in cost? Using the efficiency of a 33 mpg car, one kWh of electricity will produce 3 car miles for an equivalent electric car. Changing these numbers into cost values, an internal combustion vehicle cost 10.6 cents per mile to drive while the electric car costs 5.6 cents per mile. These numbers are for gasoline at $3.50 per gallon and for PV electricity at 16.8 cents per kWh (see Figures 4 and 5). Thus, the cost to drive the PV powered electric car is less than half that of the gasoline car. This supplies the demand.

If Florida was to change all its small cars to electric or hybrid cars, we could save 1.8 billion gallons of gasoline. We will have to pay for small car's electricity, but this change will still save $3.2 billion in fuel costs per year. This change will also give the need for 15 billion more KWh (15 TWH) or 4 more electric power plants.

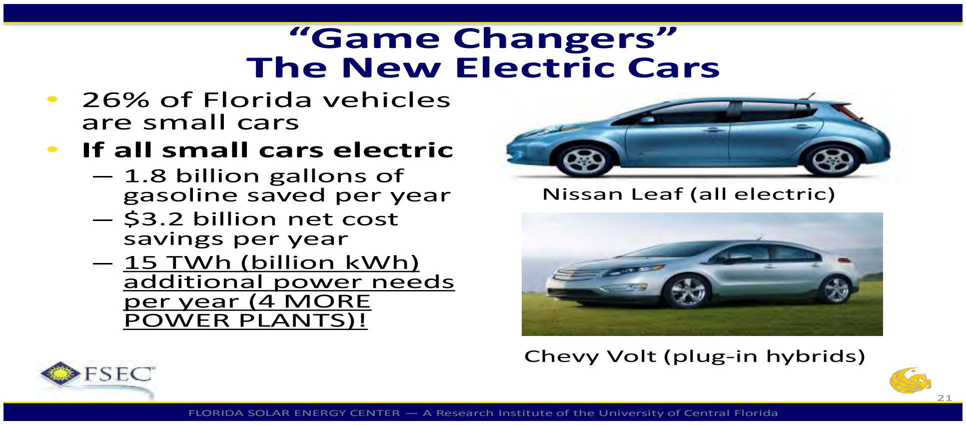

Figure 4: Electric Vehicles

Florida Photovoltaic Power is Equivalent to $1.85 Per Gallon Gasoline

	Fuel Efficiency	Fuel Price	Cost per Mile	Cost per 12,000 Miles
Gasoline Small Car	33 mpg	$3.50 per gal	10.6¢ per mile	$1,272
Electric Car	3 miles per kWh	16.8 ¢/kWh ($1.85 per gal equiv.)	5.6¢ per mile	$672

22
FLORIDA SOLAR ENERGY CENTER — A Research Institute of the University of Central Florida

Figure 5: Electric Costs

References:

1. The Solar Industries Monthly Market Monitor, PV News, Vol. 30, No. 5, May 2011.

2. U. S. Solar Market Insight, 1st Quarter 2011, Solar Energy Industry Association, April 2011.

University of Central Florida

Insight into Membrane Degradation Mechanisms Through Verification of Chemical and Mechanical Degradation Test Capabilities

PI: Darlene Slattery **Co-PIs:** Len Bonville, Marianne Rodgers

Description: The objectives of the program were to gain insight into fuel cell membrane degradation mechanisms including both chemical and mechanical degradations. In order to achieve this objective, the Membrane Electrode Assembly Durability Test System, MEADS, was verified, after which chemical degradation tests were conducted. By performing post mechanical testing and analyzing the data, the impact of accelerated degradation tests on the cell performance decay, chemical decomposition and mechanical weakening of the membranes were evaluated.

Budget: $351,518
Universities: UCF/FSEC
External Collaborators: U. S. Department of Energy

Executive Summary

This project was essentially completed by fall 2010. However, it was determined that the ability to obtain publication quality transmission electron microscopy (TEM) images would be beneficial to a better understanding of membrane degradation. Additionally, this capability would enhance the ability to obtain future funding in this field. As a result, contract funding was used to purchase a Leica Trimmer and a Leica Microtome. The trimmer is employed for rough trimming of samples and then the microtome is used to prepare the samples, which must be thinner than 100 nm in order to obtain high quality TEM images. These two instruments were installed at the Material Characterization Facility at UCF, where the TEM resides and are available to all UCF researchers.

2011 Annual Report

In order to better determine the impact of fuel cell testing on membranes; it is necessary to examine cross-sections of the tested membranes using a transmission electron microscope (TEM). The Materials Characterization Facility (MCF) at UCF has an excellent TEM but it was determined that the existing microtome, used for preparing the cross-sections, was not adequate for this purpose. This instrument must be capable of preparing slices of the sample that are 80-100 nm thick in order for the TEM to obtain clear images of fuel cell membranes. With the MCF microtome, a diamond knife could not be used and as a result slices were either too thick or were shredded. It was therefore decided that a new microtome would be purchased. It was determined that the Leica EM UC7 possessed all of the required characteristics and so was purchased under this program. It was also determined that before the microtome could be used, a trimmer was required to perform the rough trimming of the samples. Leica carried this instrument and it was purchased to be used in conjunction with the microtome. The instruments, which were installed in the MCF facility for use by all UCF faculties, can be seen below.

Florida Energy Systems Consortium

Figure 1: Leica Trimmer

Figure 2: Leica EM UC7 installed at MCF

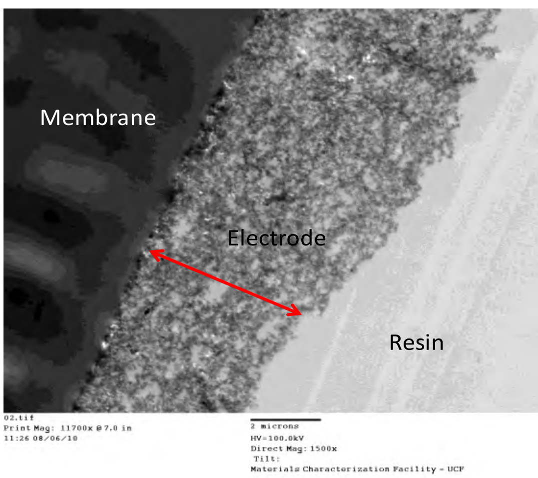

Figure 3: Partial cross-section image of an MEA

This Leica microtome provided samples that were far superior to any previously obtained with the old instrument. The capability to acquire publication quality TEM images has been greatly enhanced with the acquisition of both the trimmer and the microtome.

An example of the images obtained after sample preparation using the new instruments can be seen in Figure 3.

This project has been completed.

University of Central Florida

Integrated Florida Bio-Energy Industry

PI: Ali T-Raissi, PhD **CO-PI:** N.Z. Muradov (PhD-Chemist), D.L. Block (PhD)
Research Team: Amit Gujar (PhD-ChE), Jong Baik (PhD-ME), Nathaniel Garceau (BS-ChE) and Suzanne Fenton (PhD-ChE), Errol Hinkamp (MS-ChE)

Description: The aim of this project is to produce liquid hydrocarbon fuels (LHF) derived from Florida's biomass resources utilizing a two-step thermochemical process. In the first step, biomass is gasified with oxygen and steam to synthesis gas (syngas) comprised of mostly hydrogen and carbon monoxide. Use of oxygen for gasification of biomass allows higher overall process energy conversion efficiency to be realized as it circumvents syngas dilution with nitrogen (if air is used instead). In the second step, syngas is cleaned and then fed into a Fischer Tropsch synthesis unit that converts the synthesis gas to liquid hydrocarbon fuels containing gasoline and diesel fractions. The process can be employed with any lignocellulosic material including crop residues, forest waste, yard clippings, and energy crops. The technology also provides a means for sequestering carbon in the form of a high-value soil enhancing bio-char (*terra preta*) by simple modification of the gasification step 1.

Budget: $386,409
Universities: UCF-FSEC

Progress Summary

The aim of this project is to produce liquid hydrocarbon fuels (LHF) derived from Florida's biomass resources utilizing a two-step thermochemical process. The first step of the process comprised of a pilot-scale gasifier that was operated using pinewood charcoal as the feedstock. The gasifier operated in bottom-lit updraft mode using a mixture of oxygen and steam as oxidizing agents - introduced from the bottom of the gasifier, and the output gas exited from the top (see picture below). The main objective of the gasification experiments was to determine the effect of oxidant flow rate and inlet $[H_2O]_0/[O_2]_0$ ratio on the performance of the gasifier and quality and composition of the syngas produced.

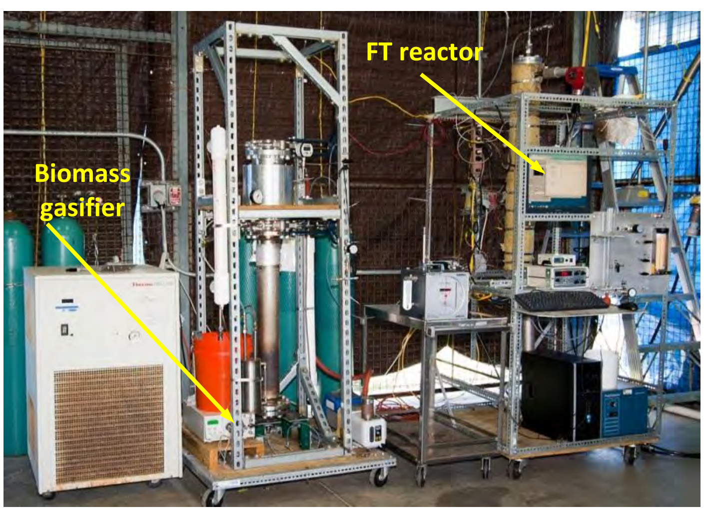

Table below presents typical experimental data collected during one integrated gasifier-Fischer Tropsch (FT) synthesis run in which the gasifier pressure was set at 100 psig and flow rates of oxygen and water were 2700 mL/min and 270 g/hr, respectively. The gasifier biomass feed consisted of a mixture of about 800g of pinewood charcoal and 131.6g of virgin pinewood pellets.

Time, min	Thru FT reactor?	%CO	%H_2	%CO_2	%CH_4	Syngas flow rate, L/min
9	NO	43.3	32.8	21.9	1.8	8.92
32	NO	40.0	28.9	25.9	5.35	9.78
46	NO	34.5	30.9	27.9	5.56	9.21
80	YES	31.0	31.8	29.6	5.60	9.16
110	YES	35.0	33.6	26.1	5.04	9.06
136	YES	38.4	29.7	24.0	6.25	8.42
155	NO	38.3	30.9	24.7	5.85	9.00
175	YES	42.6	33.0	20.1	3.32	8.30
180	YES	44.0	32.2	20.5	2.98	5.94

The second step of the process comprised of a FT reactor that was operated at 240°C temperature. A slipstream of about 1.5 L/min was diverted from the gasifier exit line and passed through the FT reactor. At the end of the run, approximately 0.53g of organic liquid product was collected. The GC-FID analysis of the condensate showed that it composed of about 33.13 wt% gasoline range (C_5-$C1_0$), 7.52 wt% kerosene/jet fuel range (C_{11}-C_{12}), 23.22 wt% diesel range (C_{13}-C_{16}), and 36.14 wt% lube oil and wax range (C_{17}-C_{26}) hydrocarbons.

2011 Annual Report

Background: The growing demand for clean renewable energy is creating market pull worldwide to develop viable environmentally benign processes for converting biomass to liquid hydrocarbon fuels (LHF). The objective of this project was to develop a viable thermochemical process for converting Florida-grown biomass to fungible liquid transportation fuels. Biomass feedstocks selected for this investigation included both lignocellulosic (*e.g.* pinewood) and aquatic (*e.g.* duckweed) species. The approach taken for processing the biomass-to-liquid fuels (BTL) involved two successive steps – 1) syngas (a mixed gas comprised of mostly hydrogen and carbon monoxide) production via gasification of biomass with steam and oxygen; 2) syngas to LHF conversion via Fischer-Tropsch (FT) synthesis. A more detailed description of the BTL process is given below.

Integrated biomass gasification and Fischer-Tropsch synthesis: Gasification coupled with Fischer-Tropsch (FT) synthesis offers many advantages. For one, any source of biomass can be used in the process (*e.g.,* lignocellulosic materials such as crop residues, forest waste, yard clippings, energy crops; as well as the aquatic biomass. For another, the process generates a range of liquid hydrocarbons that can be easily upgraded to fungible transportation fuels (*e.g.,* gasoline, diesel, aviation fuels, etc.) using conventional refining operations such as distillation, hydrocracking, etc.

This is a two-step process. In the first step, biomass is gasified with oxygen and steam to synthesis gas (syngas) comprised of mostly hydrogen and carbon monoxide. Use of oxygen for gasification of biomass allows higher overall process energy conversion efficiency to be realized as it circumvents syngas dilution with nitrogen (if air is used instead). In the second step, syngas is cleaned and then fed into a FT synthesis unit that converts the synthesis gas to LHF containing gasoline and diesel fractions.

The biomass gasification experiments employed several different gasifiers – all designed, fabricated and tested at the Florida Solar Energy Center (FSEC). In order to identify the best gasification configuration, operational parameters (*e.g.,* temperature, pressure, steam/oxygen ratio, rate of biomass gasification, etc.) for each reactor design were varied and their effect on the amount and composition of syngas (especially H_2/CO ratio), and the extent of CO_2 generated were determined. It was found that the H_2/CO ratio and the rate of biomass gasification increase monotonically as a function of $[H_2O]/[O_2]$ ratio (at a fixed O_2 flow rate). Also, there appeared to be an optimum $[H_2O]/[O_2]$ ratio for which the CO_2 concentration in the syngas was minimum.

The FT synthesis of liquid hydrocarbon fuels was conducted in a number of fixed-bed reactor designs. FT reactors used especially prepared (at FSEC) catalysts including, among others: K-promoted and silica-supported iron, silica-supported cobalt, molybdenum-Zeolite Y. It was found that Fe-based catalysts produced LHF (mainly, C_5-C_{22} hydrocarbons) rich in unsaturated hydrocarbons. The unsaturated hydrocarbons tend to adversely affect the long-term stability of the fuel.

Unlike iron-based catalysts, the cobalt-based catalysts produce mostly straight chain alkanes that remain stable for much longer period of time. Catalyst combinations such as Fe+Ni-Mo/alumina, Fe+H^+-ZSM-5 were also evaluated for their potential to improve the quality of LHF produced. Also, issues related to heat and mass transfer in the FT reactors were investigated. Finally, a new FT reactor design having radial flow configuration was built and tested showing improved heat and mass transfer characteristics.

A fully integrated and instrumented (using Lab-View platform) pilot-scale BTL system was built and tested. The unit operates continuously and is comprised of an oxygen-blown gasifier, a cyclone separator, syngas purification and conditioning unit, a steam generator, an FT synthesis reactor, and a product collection system. The integrated system employed a bottom-lit updraft gasifier, and an FT radial flow reactor loaded with silica-supported cobalt (Co/silica) catalyst. The liquid product collected after a typical run consisted of a hydrocarbon fraction, mainly, C_6-C_{24} saturated hydrocarbons and excess water. Also, the integrated unit did produce a small amount of higher molecular weight waxy hydrocarbon compound (see picture below).

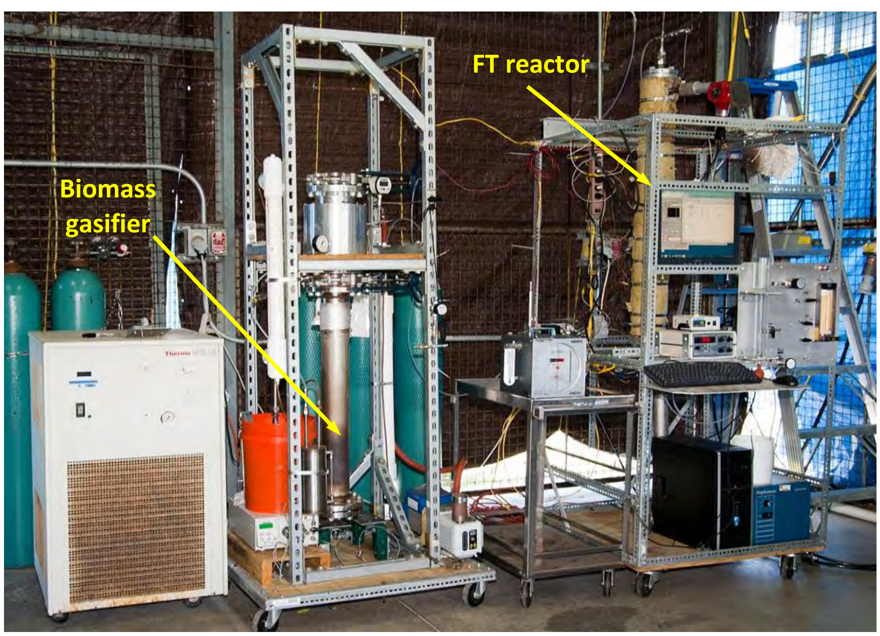

Results and Discussion: In a typical run, the integrated gasifier-Fischer Tropsch (FT) synthesis reactor operated at a system pressure of 100 psig. The flow rates of oxygen and water entering the gasifier were 2700 mL/min and 270 g/hr, respectively. The biomass was fed continuously to the gasifier and consisted of about 800g of pinewood charcoal mixed with 131.6g of virgin pinewood pellets. The data obtained are shown below.

Run time, min	Thru FT reactor?	%CO	$\%H_2$	$\%CO_2$	$\%CH_4$	Syngas flow rate, L/min
9	NO	43.3	32.8	21.9	1.8	8.92
32	NO	40.0	28.9	25.9	5.35	9.78
46	NO	34.5	30.9	27.9	5.56	9.21
80	YES	31.0	31.8	29.6	5.60	9.16
110	YES	35.0	33.6	26.1	5.04	9.06
136	YES	38.4	29.7	24.0	6.25	8.42
155	NO	38.3	30.9	24.7	5.85	9.00
175	YES	42.6	33.0	20.1	3.32	8.30

The first entry to the table (at 9 min) was at atmospheric pressure and the rest were at 100 psig. The run was terminated at 180 min through since the output gas flow rate (as well as pressure) began to drop indicating that the fuel was exhausted. The profile of gasifier internal pressure is shown below.

The second step in the process involves Fischer-Tropsch (FT) treatment of the syngas generated by the gasifier. The FT reactor operated at 240°C temperature. A slipstream of about 1.5 L/min was diverted from the gasifier exit line and passed through the FT reactor. At the end of the experiment, approximately 0.53g of organic liquid product was collected.

The GC-FID analysis of the condensate showed that it composed of about 33.13 wt% gasoline range (C_5-$C1_0$), 7.52 wt% kerosene/jet fuel range (C_{11}-C_{12}), 23.22 wt% diesel range (C_{13}-C_{16}), and 36.14 wt% lube oil and wax range (C_{17}-C_{26}) hydrocarbons.

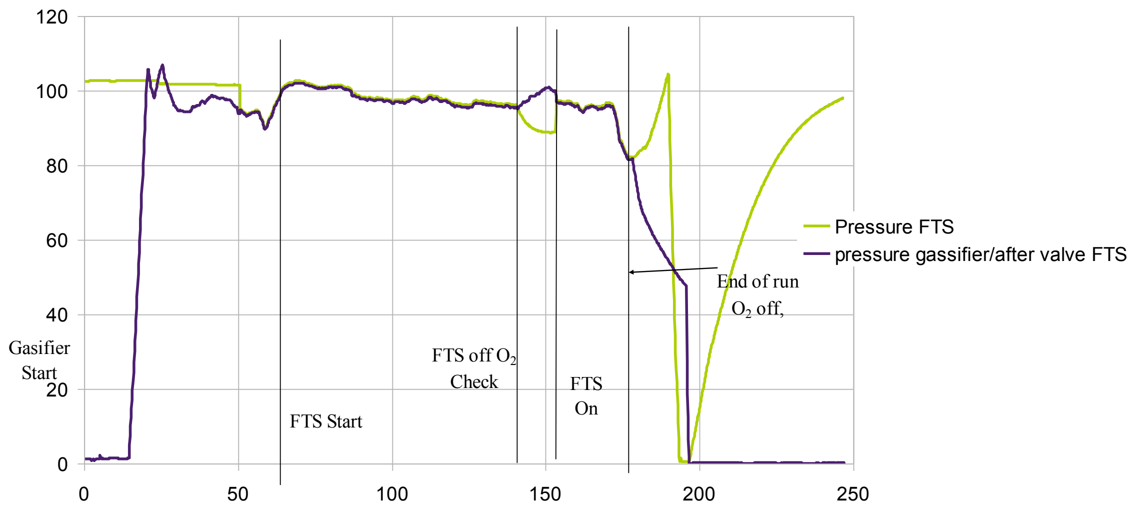

Thus, we were able to demonstrate production of LHF (especially, gasoline and diesel range synthetic hydrocarbon fuels) directly from biomass derived syngas. The following Figure depicts the raw products of Fischer-Tropsch synthesis of pinewood derived syngas obtained during the operation of the pilot scale unit. The upper layer on the left photo is hydrocarbons, and the lower layer – water. Right Photo shows waxy product obtained during FT reaction.

Large-Scale BTL Plant Design, Modeling and Costing: Based on the extensive experimental data collected, and using the AspenPlus™ chemical process simulation platform, a preliminary flowsheet of a full-scale biomass-to-liquid fuel plant was prepared and its economics evaluated. The Aspen generated output for a single set of non-optimized operating conditions was used to conduct order-of-magnitude estimates of the total plant cost and from that, the fully burdened cost of the fuel generated. Table below depicts the assumptions used for the cost analysis.

Process	
Design capacity (kg FT fuel produced/yr)	93,688,930
Capacity factor	0.90
Actual FT fuel production (kg/yr)	84,320,037
Financial	
Start-up year	2025
Analysis period (yrs)	15
Plant life (yrs)	25
Depreciation type	MACRS
Depreciation period (yrs)	20
% Equity financing	100
Decommissioning costs (% deprec capital)	10
Salvage value (% total capital)	10
Inflation rate (%)	1.90
After tax Real IRR (%)	10
Total tax rate (%)	38.9

Capital Costs	
Total direct & indirect depreciable (2005$)	310,850,202
Total non-depreciable (2005 $)	250,000
Total Capital Investment (TCI) (2005 $)	311,050,000
Annual Operating Costs	
Total plant staff	50
$/man-hr (including overhead)	50
Prop tax & insurance rate (% TCI)	2
Maintenance (% dir cap cost)	0.50
Waste treatment & disposal (%TCI)	1.0
Other raw material costs (catalyst, boiler chem., cooling tower chem.) $/yr	5,000,000
Biomass feed, $/ton	163
Electricity (credit) $/kWh	0.056

Based on this analysis, the integrated biomass gasification and FT synthesis process is thermodynamically and economically feasible with an overall efficiency of about 40% based on polygeneration of fuel, heat and power. Simulation results indicate that the biomass feedstock costs make up about 54.4% of the total cost of liquid fuel produced. At biomass cost of $163/ton and plant production capacity of 84,320 metric ton per year, the cost of LHF would be about $7 per gallon. If lower cost biomass feedstocks are available, a fuel cost in the range of $3/gallon can be realized; as shown in the Table below.

Cost component	Cost ($/kg of FT fuel produced)	% of total cost
Capital costs	0.81	39.3
Fixed O & M	0.18	8.6
Feedstock	1.12	54.4
Other raw materials	0.06	3.0
Byproduct credits - electricity generation	-0.13	-6.5
Other variable costs	0.02	1.2
Synfuel cost (at the gate)	***$2.06***	Per kg
	$7.00	Per gallon

Acknowledgements: Funding for this project was provided by a grant from the Florida Department of Agriculture & Consumer Services (FL DACS) – Farm-to-Fuel program. Additional funds were made available by the UCF-FSEC and with indirect support (matching funds) of the Florida Hydrogen Initiative (FHI), Chevron Technology Ventures (CTV) and Florida Energy Systems Consortium (FESC). We thank Dr. Bill Grieco of the PetroAlgae, Inc. for providing duckweed samples used in some of the pyrolysis and gasification experiments reported here. We are also grateful to the both past and present (see picture below) Florida Agriculture Commissioners and especially to Mr. Jay Levenstein, Deputy Commissioner at the Florida Department of Agriculture & Consumer Services.

Nazim Muradov, Principal Research Scientist at the Florida Solar Energy Center, shows Florida Agriculture Commissioner Adam Putnam, biomass that can be made into diesel fuel.
Photo credit: Malcolm Denemark, FLORIDA TODAY

University of Central Florida

PV Devices Research and Development Laboratory

PI: Robert Reedy **Co-PI:** Nicoleta Hickman, Neelkanth Dhere,
Student: Kristopher Davis, Ph. D, CREOL-UCF

Description: The goal from this project is to develop and equip a PV devices R & D laboratory which would then be open to industry, research institutions and academic partners for the purposes of planning, designing, deploying and operating PV systems. The new PV Devices Research and Development Laboratory is a comprehensive suite of scientific tools for the fabrication and characterization of materials and PV devices. The laboratory is located in a new PV laboratory room at FSEC and is designed specifically to reduce time delays associated with transferring technology from the academic research laboratory to industry. Furthermore, the PV laboratory will also facilitate undergraduate and graduate internship programs to train chemists, physicists and engineers in photovoltaic processing, characterization and testing.

Budget: $450,250
Universities: UCF/FSEC

Progress Summary

The goal of this project is to develop and equip a photovoltaic devices laboratory which would then be open to industry, research institutions and academic partners for the purposes of planning, designing, deploying and operating PV systems. Although reliable PV systems are commercially available and widely deployed, further development of PV technology is crucial to enable PV to become a major source of electricity. The current price of PV systems is not low enough for PV electricity to compete with the price of peak power in grid-connected applications and with alternatives like diesel generators in stand-alone applications. It also cannot rival consumer or wholesale electricity prices. A drastic further reduction of turn-key system prices is therefore needed. For these reasons, research and development is crucial for the advancement of PV. Performing joint PV research and addressing well-chosen research issues can play an important role in achieving the critical mass and effectiveness required to meet the sector’s ambitions for technology implementation and industry competitiveness.

In the FSEC PV Devices Research and Development laboratory, researchers collaborate with other research teams in using established fabrication and characterization techniques and to develop new in-situ diagnostics tailored for the specific growth and processing steps used in PV manufacturing. The following customized capabilities distinguish FSEC’s Devices Research and Development PV Laboratory:

- Dimatix nanomaterials injector printing system,
- Two plasma chemical vapor deposition systems for fabrication of nanorods and controlled size and shape nanostructures,
- Organic/inorganic solar cell fabrication unit using fully enclosed XYZ tabletop normal and ultrasonic spraying system,
- Customized Oriel external and internal quantum efficiency system,
- Oriel Class 3A solar simulator for characterization of novel developed solar cells,
- UV-Vis-NIR spectrophotometers and refractometers for optical analysis and in-situ electro-optical characterization techniques tailored for the specific growth and processing steps used in

PV manufacturing like spectroscopic ellipsometry, photoluminescence, photocurrent decay, fourier transform infrared, and Ramen scattering, and indoor and outdoor I-V curve tracers.

2011 Annual Report

The systems acquired for the PV lab and configured to operate are described in detail as follows.

1. Customized Oriel Quantum Efficiency System

The quantum efficiency (QE) system is an essential tool for any laboratory working on PV materials and devices. With the help of Oriel's product engineers, FSEC's researchers have configured this system to measure internal quantum efficiency (IQE). The difference between IQE and EQE is that IQE measurements account for any EM radiation reflected from or transmitted through the PV cell under test. By doing this, one can infer more about the internal workings of the active semiconductor layer, without concern regarding the cell's external optical properties (e.g. anti-reflection coatings). This allows the determination of whether bad performance comes from the active semiconductor itself or simply from high reflection losses at the surface of the cell.

The configuration and operation of this system has included many tasks, including installation of the individual components, optical beam alignment, integration of the LabView based software, several rounds of troubleshooting relating to both hardware and software complications, procedure development, adaptation of test procedures for novel materials and device architectures (e.g. organic PV, multi-junction devices), and development of analytical techniques for processing data. A large part of the effort was placed in customizing this system to measure transmission, absorption, and reflection
measurements of samples, which is required for IQE. Working with Sphere Optics, a manufacturer of integrating spheres, the research group was successful in achieving this new functionality.

Customized Oriel Quantum Efficiency System

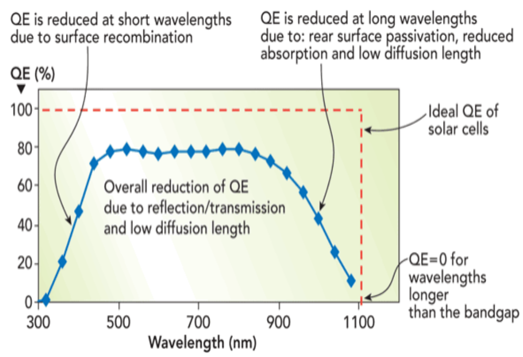

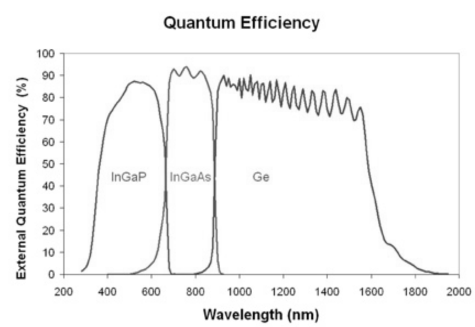

2. Oriel Class 3A Solar Simulator

In the context of PV materials and device research, a solar simulator allows for a dependable measure of device performance under broadband radiation that is spectrally similar to that coming from the sun. The configuration and operation of this system has included the fabrication of a suitable structure for safely mounting the simulator on the laboratory bench, installing individual components (e.g. light source, power supplies, optical filters, etc.), verifying proper beam alignment and light throughput, and testing the unit with actual PV cells with known current-voltage characteristics. The Oriel Sol3A simulator is certified to IEC 60904-9 Edition 2 (2007), JIS C 8912, and ASTM E 927-05 standards for Spectral

Match, Non-Uniformity of Irradiance, and Temporal Instability of Irradiance. The Oriel Sol3A simulator use a single lamp design to meet all three performance criteria without compromising the 1 Sun output power and, thus, providing true Class AAA performance. The Oriel Sol3A uses a black non-reflective finish to minimize stray light and incorporates captive screws for all panels requiring user access to facilitate lamp replacement, alignment, and filter changes. See below figure for device and irradiance plot.

Orial Class 3A Solar Simulator

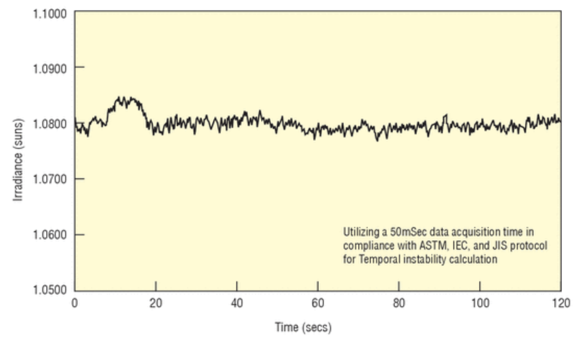

3. Laurell Technologies Spin Processor

Spin coating systems are a common tool in semiconductor fabrication labs and facilities. They allow for a controlled deposition of liquid phase materials. The Laurell Technologies system features an automated dispense system, which allows for better control of the fluid during deposition, therefore better control of the final thickness. This control is very important for PV devices that feature individual layers smaller than 100 nm. The configuration and operation of this system has involved the fabrication of a structure to house the system, installation of individual components (e.g. vacuum pump for the substrate chuck, compressed nitrogen cylinder and regulator for system's pressure inlet), integration of the system software and final verification of proper operation. This system has been used for thin film deposition with different composition, substrates, and microstructures. Some of the key features of the system are:

- Organic and inorganic thin films can be deposited onto any kind of substrates,
- The deposited film can be dense or porous after sintering, depending on requirements for the film,
- The deposition rate and the spinning rate are high,
- The process can be done in under a minute.

Laurel Spin Processor

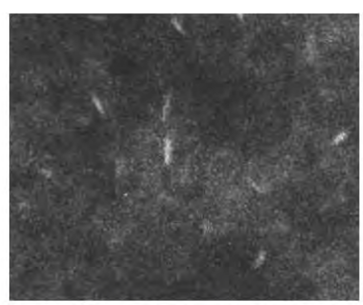

Structure of the PSDOT/PSS doped with ZnO nanoparticle fabricated with the spin coating system

4. Dimatix DMP-2831 Materials Printing System

The largest and most expensive item of fabrication equipment is the material printing system (Dimatix, Inc). It is a system used for inkjet- printed quantum dot and nanostructure hybrid PV and TE materials and devices. The system provides a high degree of fabrication accuracy and reliability of fabrication when operated and maintained correctly.

The DMP-2831 is a state of the art printing system which will generate new research capabilities that include experiments with inkjet deposition of organic semiconductors, inorganic solution based semiconductors, and patterned conductive layers. The configuration and operation of this printing system has included the installation of individual components, installation and operation of the system software, fluid transfer to printer cartridge, and troubleshooting to overcome non-jetting nozzles.

5. Spraying system

Inkjet printing is used to create the actual solar absorber, which is the layer in a solar cell in which the sunlight's energy generates free electrons. The inkjet printing technique can be applied to any thin-film materials or organic photovoltaics. For example, cadmium telluride, Si, organic-inorganic materials are absorber layer materials which are being developed for deposition by a liquid precursor. Also, nanoparticulate-based ink is spray-deposited to form a film. Work has successfully produced optically dense thick films—up to 10 micrometers with no cracks. Many solar cell technologies collect freed electrons using a thin layer of transparent conducting oxide rather than metallic grid lines. This work uses special inks, fabricated in our laboratory with spray deposition, to lay down thin, high-quality transparent graphene and carbon nanotubes based layers. Continuing work is expected to improve this technique so that conductivities will rival those of conventionally deposited.

Inkjet Sprayer

Structure of the porous nanoparticle of TiO_2 fabricated with the spraying system

University of Central Florida

PV Energy Conversion and System Integration

PI: I. Batarseh **Co-PIs:** J. Shen, Z. Qu, X. Wu, W. Mikhael, L. Chow
Post Docs: H. Hu (PhD)
Students: Kejiu Zhang (PhD), Souhaib Harb (PhD), Lin Chen (PhD)
Karthik Padmanabhan (PhD), Xiang Fang (PhD), Ala Alsaeed (PhD)

Description: The objective of this project is to develop a system-driven Plug'N'Gen solar power system demonstrating architecture of decentralized, low-cost, mass-produced, PV panel-mounted micro-inverters. This system will be able to compete with today's centralized multi-kW PV inverters that require cost prohibitive professional installation. The project tasks are: 1) novel inverter topology and control concepts; 2) advanced digital control algorithms; 3) SmartTie interface with the utility grid; and 4) low cost and ultra-compact PV inverter in package.

Budget: $1,267,000
Universities: UCF
External Collaborators: U. S. Department of Energy awarded the UCF PIs a two year $1,400,000 project (DE-EE003176) called "Photovoltaic Power Electronics Initiative (PERI)"

Progress Summary

The focus of this period was on developing very high efficiency LLC resonant DC/DC converter stage for the PV inverters.

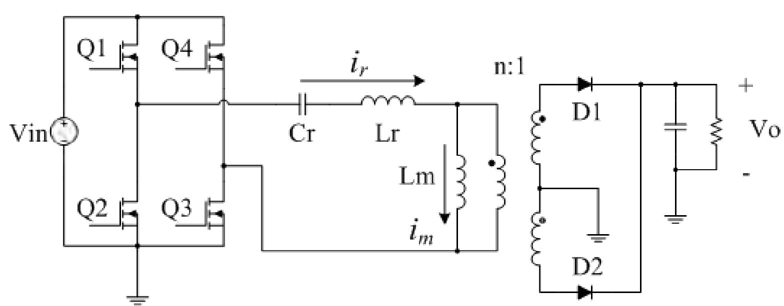

LLC is a 3-resonant-component converter topology with high efficiency and high power density. It has advantages of achieving ZVS for wide input voltage and load range, which makes it ideal candidate for PV applications. LLC's operation is complicated. A systematic analysis and modeling based on its operating modes are proposed and verified by experiments. The model provides high accuracy in DC gain prediction comparing to traditional approaches (FHA method). And the model is used to optimize LLC design. A modified LLC topology with dual transformers is proposed. The modified topology has better efficiency than traditional one. A prototype board was built to perform comparative tests.

LLC optimal design is to find the circuit parameters that minimize the power loss while maintaining a desired DC gain level to adapt the wide input range. An optimal design procedure is developed based on the mode model. The experiments validate our LLC model study and show promising results of the dual-T LLC topology. A power loss model will be built to further improve the converter efficiency. Based on these results, the circuit for its implementation in the mico-inverter prototype will be finalized.

Title: Photovoltaic Power Electronics Initiative (PERI)	Agency DOE	Period of Performance 24 months	Funding awarded $1,400,000

2011 Annual Report

Research on high step-up front-end DC/DC converter

Description

Based on extensive literature survey on the high step-up DC/DC converter, achieving high conversion efficiency with a high voltage gain presents the greatest challenge for non-isolated DC/DC topologies, which either operate with an extreme duty-ratio or result in high cost or low efficiency. Isolated topologies offer a more attractive solution. Another benefit of the isolated topologies is that it is easier to implement dual grounding for PV applications. To date, numerous isolated DC/DC converter topologies have been proposed in the literature, which can be categorized into six families: full bridge, half bridge, push-pull, resonant, forward and flyback. We have selected typical designs from each topology family to compare their efficiency with modeling approaches. Table 2 shows the peak efficiency numbers for different topologies.

Table 2: Comparison on High step-up DC/DC converters

DC/DC topologies	***Power rating(W)***	***Input voltage(V)***	***Output voltage(V)***	***Peak efficiency(%)***
Full bridge phase-shift	1kW	48	380	96%
Current fed half -bridge	200W	24	200	95.8
Push-pull	1.5kW	35V	350	96.5
Forward	1.0kW	36	380	97.3
Flyback	260W	36V	350	97

Approach

LLC converter offers soft switching and high switching frequency, and has the potential to achieve both high efficiency and high power density. LLC converter could be a very promising candidate for this project due to these favorable features. However, there are still several shortcomings to be overcome:

(1) There is no accurate LLC converter analytical model to guide design optimization. Fundamental harmonic approximation (FHA) is a widely used method in LLC analysis and design, which simply considers all current/voltage as single frequency sinusoidal waveforms. However, it's inaccurate when frequency varies in a wide range;

(2) There are conflicting requirements between efficiency and wide input voltage range.

An accurate LLC converter model is developed using numeric method and verified by experiment. Fig.2 shows the model verification and comparison results based on 250W design. It indicates that the developed model matches the experimental results very well.

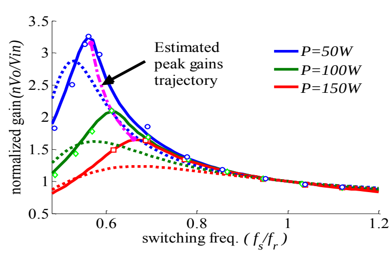

Fig.2: Comparison between mode model (solid lines), FHA (dash lines), estimated peak gains (dash-dot line) and experiment (markers)

LLC converter has 3 resonant components. It proved to be a significant challenge on how to optimize these three components. We devoted much of our effort to analyzing different LLC operation modes. From the LLC mode analysis, we learned that the resonant current level is related to the parameter Lm/n: the larger the Lm/n value (n stands for turn-ratio of transformer), the lower the resonant current is, which is preferable since it indicates smaller conduction loss. In this way, the optimization design is simplified as finding the maximum Lm/n while meeting the DC gain requirement.

A modified LLC converter, shown in Fig.3, is proposed to achieve the high efficiency, while maintaining wide DC gain range. A comparative study has been carried out between the proposed topology with the traditional design (conventional LLC converter shown in Fig.4). Two converters were optimally designed based on the aforementioned optimal design approach. Fig.5 shows the efficiency improvement by the proposed topology.

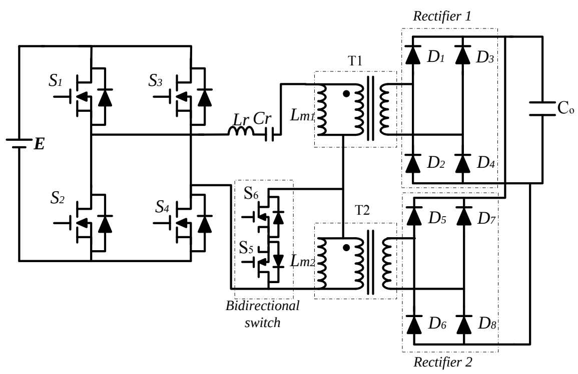

Fig.3: Modified LLC converter

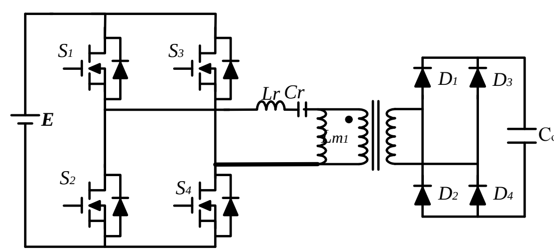

Fig.4: Traditional LLC converter

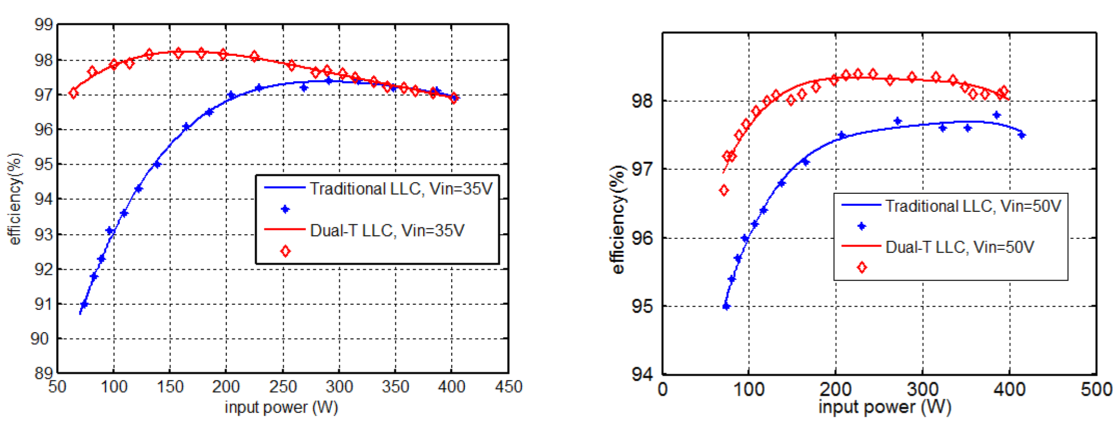

(a)Vin=35V (b) Vin=50V

Fig.5: Efficiency comparison between two LLC converters

FESC
Florida Energy Systems Consortium

University of Central Florida

PV Power Generation Using Plug-in Hybrid Vehicles as Energy Storage

PI: J. Shen **Co-PIs:** I. Batarseh
Students: Ross Kerley (PhD), Chris Hamilton (MS)

Description: The objective of this project is to develop and demonstrate an alternative PV power generation architecture that uses plug-in hybrid vehicle as the energy storage and transfer element with a total system cost target of $3.50/W. The tasks include developing efficient, reliable, and inexpensive maximum power tracking DC/DC battery chargers and 3-phase converters. A 10kW demonstration solar carport charging station was built on UCF campus. A plug-in hybrid vehicle with a 25kWh battery bank (battery-only driving range of 50-100 miles) and onboard bidirectional AC charging system will be demonstrated

Budget: $380,816
Universities: UCF
External Collaborators: City of Tavares, FL

Progress Summary

Research Objectives for Current Reporting Period: The main research objectives for the current reporting period include the development of power electronics hardware and fine tuning of control software.

Progress Made Toward Objectives During Reporting Period: A 10kW smart solar plug-in electric vehicle charging station was constructed on UCF campus. The PHEV Smart Solar Carport is configured as two 5 kilowatt systems providing a total power output of 10 kilowatts. Most PHEVs currently available today are configured to receive standard "household" 120 volt Alternating Current (AC), so an inverter converts the DC into the required AC power for the vehicle chargers. The new system not only offers this feature but also facilitate future deployment of experimental technologies that will interface the DC produced by the photovoltaic modules directly with the DC batteries in the electric vehicles. This would allow direct DC transfer to the vehicle batteries, thereby eliminating losses associated with converting the DC to AC, and then back to DC power. A unique control strategy is implemented, allowing efficient energy transfer while reducing the conversion stages between the source and the load. All of the pedestals are reconfigurable and include provisions to accommodate future vehicle charging configurations. The solar carport system is "grid interactive" in that the inverters produce AC voltage that is synchronized with the electrical grid. This means that power produced from the PV panels in excess of what is needed to charge the electric vehicles will "go back" into the University's electrical grid. This allows the campus grid to act as an energy "bank" in which the excess capacity from the solar carport can be used to power other electrical demands on the campus. The interactive system also allows for non-sunlit period vehicle charging. On an annual net metering basis, the carport is anticipated to be a net exporter of power to the grid as there will be a significant number of sunlit hours during a year when the majority of electric vehicles parked at the facility are fully charged, and during semester breaks and weekends. A communication link will be established between the system and the power grid to facilitate intelligent control.

Several hardware prototypes have been built to facilitate the three-way energy flow control. Final prototyping for the DC/DC converter is shown here. Each converter consists of a power board, a power supply board, and a controller board. The power supply board is designed to supply 12V from an input between 100V and 400V. The controller board is a generalized design with built-in sensing amplifiers. These boards are mounted vertically in the power board of each DC/DC converter included in the carport charging station. In order to increase the efficiency, soft switching was implemented in both converters (1.2kW solar DC/DC and 4kW DC/DC converters). These prototypes operate at a high overall efficiency (above 95%). Research activities for the next reporting period will focus on fine tuning of the hardware and the software control algorithms, and make efficiency comparison between the new system and the convention configuration over a wide range of conditions.

2011 Annual Report

I. Introduction

Photovoltaic modules have become a viable renewable energy source for energy systems in communications, commercial, and residential applications. Plug-in electric or hybrid vehicles appear in the market as an emerging technology to reduce carbon emissions and improve energy efficiency. PV modules and electric vehicles interact with the power grid as energy source and energy sink elements, respectively. However, little was reported on energy conversion systems featuring a three-way energy flow among the power grid, PV modules, and electric vehicles. The research described in this report examined the concept and devised a system to test and demonstrate the concept.

II. System Overview

This three-port system is designed as a carport, providing shade for two parking spaces. This prototype system consists of four strings of six 200W panels each. Each string yields a maximum power of 1.2 kW, while the whole system yields a maximum solar power of 4.8 kW. The system supports up to two 4 kW electric vehicle chargers in the system. Any surplus or deficit of power is accounted for by the grid through a grid-tied inverter or rectifier, respectively. This overall system is shown in Figure 1. The carport could be used to charge any electric vehicle with a battery bank less than 216V.

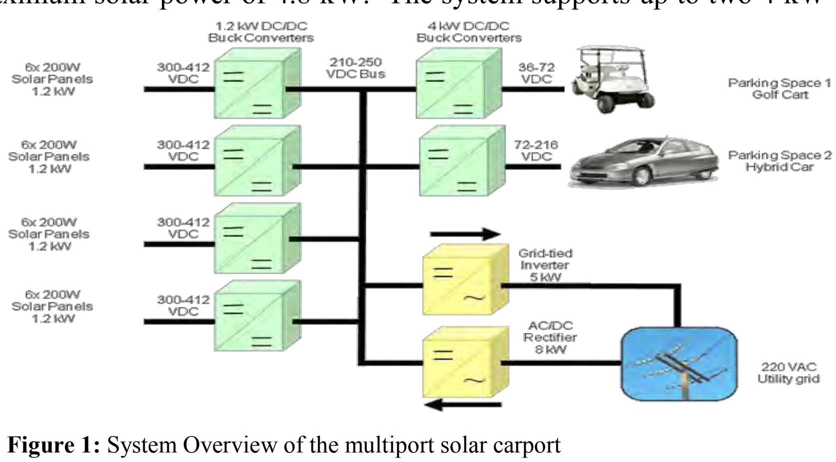

Figure 1: System Overview of the multiport solar carport

The different modules of the carport system are all connected through a common DC bus.

This bus is both a means of transmitting power, and control. The DC bus voltage is allowed to change depending on the power supply and consumption in the system. Each module is programmed to interact with the bus, varying its power with the bus voltage. For example, this droop behavior causes the battery chargers to reduce their output if the bus voltage falls, and causes the inverter to pull power from the bus if the voltage rises far enough.

III. Progress Overview

Recent progress in the solar carport project was in hardware, software, and testing of both together. Hardware progress includes testing the solar converters and battery chargers in series, and prototyping the Ground Fault Interrupter system. A safe GFI is necessary to protect people and equipment

Software progress includes development and testing of the droop control algorithm. This algorithm regulates all power electronics in the carport system. The droop control algorithm has been simulated in MATLAB. Control laws have been implemented and tested for the solar converters and battery chargers.

IV. Hardware Progress

The power converters in the solar carport have been designed, built and tested. First the solar and battery charger converters were tested at various power levels, and then they were tested in series. These tests were conducted to measure the total system efficiency.

Testing the solar converter alone yielded the efficiency data in Table 1. This shows a peak efficiency of 96.76% with 1060W in, 1025W out. Similar data was collected for the battery charger, but only at the same power levels. Full 4kW testing has not been performed yet.

Vin	Iin	Vout	Iout	Pin	Pout	Ploss	Efficiency
329.94	0.32	208.17	0.38	110	79	28	73.83
329.91	0.56	208.39	0.76	190	159	26	85.95
329.89	0.8	208.37	1.14	270	237	28	89.43
329.88	1.05	207.64	1.5	350	311	34	90.14
329.87	1.29	207.22	1.87	430	387	39	90.85
329.86	1.51	207.05	2.21	500	457	42	91.58
329.84	2	206.74	2.99	660	618	42	93.64
329.82	2.45	206.41	3.73	810	770	37	95.42
329.82	2.47	206.36	3.77	820	778	37	95.46
329.82	2.48	206.34	3.78	820	780	37	95.47
329.8	2.93	206.49	4.53	970	934	34	96.49
329.8	3.21	206.44	4.97	1060	1025	32	96.97
329.78	3.69	206.82	5.7	1220	1178	38	96.88
329.78	3.72	206.82	5.74	1230	1188	38	96.9
329.77	3.96	206.97	6.1	1310	1262	43	96.7

Table 1: Solar Converter Efficiency

The buck topology of these two converters makes use of Zero-Voltage Transition PWM soft-switching. This auxiliary circuit provides an alternative power path that reduces switching losses and voltage ringing, even under high power situations. Simulations in Pspice showed that there is approximately a 5% increase with the ZVT topology over the standard buck converter.

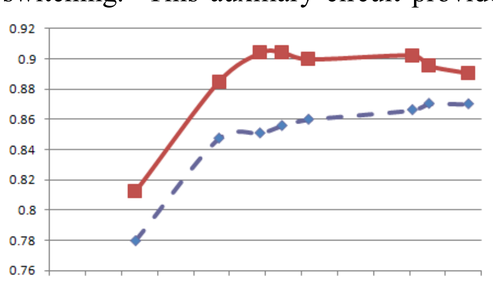

Figure 5: Efficieny curve of cascaded converters (top) vs typical setup (bottom)

Cascading the two converters allowed for testing of the efficiency and of the algorithm effectiveness. The efficiency results have been compared to a COTS grid-tie inverter and grid-tie battery charger. This experimental carport project exceeds the efficiency of a COTS system at all power levels. These preliminary results show that this DC/DC/DC conversion yields a significant increase in efficiency over the traditional DC/AC/DC conversion.

V. Controls Progress

Most of the control loops have been tested. On the solar converter, maximum power point tracking has been implemented. It has been tested to be resilient to noise and false readings. In addition to solar MPPT, the droop control laws have been tested on the solar converter and charger. The laws allow stable current sharing between converters. One additional control feature is phase interleaving in the charger.

Solar MPPT was tested using a solar array simulator configured as a 54W solar panel. MPPT runs at 10Hz with 1.0V step size. These values were optimized through testing so that the algorithm doesn't misstep on the power curve.

Droop control was tested similar to the cascaded hardware test. Two chargers were connected to the output of a solar converter to demonstrate current sharing. The solar converter was supplied by a solar array simulator and MPPT was enabled. Several tests were performed to verify current sharing between two loads. The test displayed here, in Figure 3, demonstrates what happens when a load is suddenly reduced. Battery 1 current, in orange, is reduced to zero. As a result, the bus voltage increases. Consequently the battery 2 current, in green, rises. This test demonstrates that multiple loads can share a limited amount of renewable energy using the droop control algorithm.

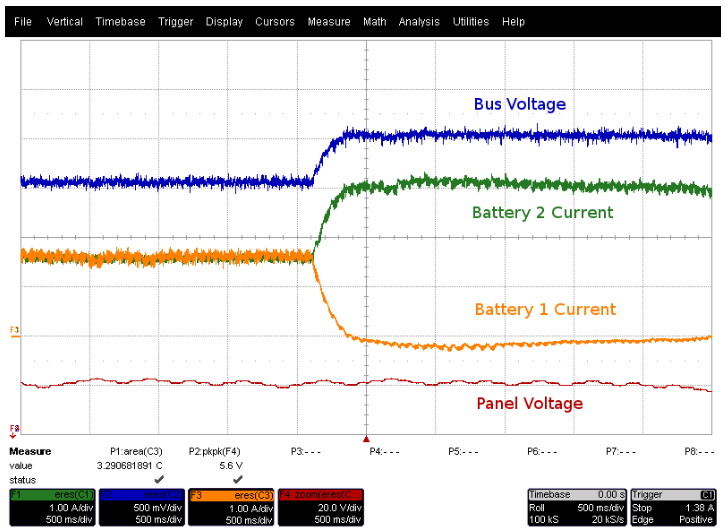

Figure 3: Droop Current Sharing

The 4kW chargers are each two buck converters in one, which allows the use of the same PCB for two solar converters. In the 4kW charger, the two buck converters can be individually controlled. This allows interleaving which reduces overall voltage and current ripple in the system. Effectively, this eliminates harmonics at the 50kHz switching frequency, only leaving those above it.

VI. Conclusion

This solar carport system has been tested at the module level. The solar converters and EV chargers are capable of safe and controlled operation with the droop algorithm and common DC bus. Additional research is necessary to develop a bidirectional DC/AC inverter, or to further the research in having a separate rectifier and inverter setup. These components would all need to have the droop control laws programmed and tested.

University of Central Florida

Research to Improve Photovoltaic (PV) Cell Efficiency by Hybrid Combination of PV and Thermoelectric Cell Elements

PIs: Nicoleta Sorloaica-Hickman, Robert Reedy
Student: Kris Davis

Description: Photovoltaic/thermoelectric (PV/TE) cell integration is a promising technology to improved performance and increase the cell life of PV cells. The TE element can be used to cool and heat the PV element, which increases the PV efficiency for applications in real-world conditions. Conversely, the TE materials can be optimized to convert heat dissipated by the PV element into useful electric energy, particularly in locations where the PV cell experiences large temperature gradients, i.e. use the thermoelectric module for cooling, heating and energy generation depending on the ambient weather conditions. Thus, the goal of this research effort is to research and develop nanoscale design of efficient thermoelectric material through a fundamental understanding of the materials properties and to design and build a photovoltaic thermoelectric (PV/TE) hybrid system.

Budget: $167,820
Universities: UCF/FSEC

Progress Summary

Photovoltaic/Optical/Thermoelectric Device- Unconventional architectures for low cost solar device with high efficiency due to the light capture and conversion

Thus, the goal of this research effort is to research and develop nanoscale design of efficient thermoelectric material through a fundamental understanding of the materials properties and to design and build a photovoltaic thermoelectric (PV/TE) hybrid system.

The realization of a high efficiency/low cost solar hybrid device which is easily manufacturable is one of the defining problems of photovoltaics. Our innovation is to design an integrated optical/PV cell hybrid system allowing efficiency improvements while decreasing the costs, and hence expand the applications for solar energy. It utilizes a design approach which focuses first on performance, enabling the use of old or new photovoltaic materials. The flexibility of these architectures allows a wide portal to accommodate new breakthrough concepts because the device accepts light at wide angles from a large fraction of the sky and it is therefore able to capture most of the diffuse light, which makes up ~10% of the incident power in the solar spectrum.

The PV device consists of many cylindrical cells imbedded into a polymeric matrix with nanoparticles which scatter the light back into the cells. The key optical elements which enhance the light capture are: light trapped by the glass/polymer fiber, light transmitted through the transparent electrodes (ITO and graphene), light absorbed and scattered by the nanoparticles imbedded into the polymeric matrix and, light reflected back into the device by the metallic substrate.

The key electrical elements which enhance the light conversion are photo-excited electrons and holes traveling very short distances before being collected by the electrodes. This concept could decrease the electronic recombination caused by impurities, high anti-reflection and high surface energy which could increase EQE.

FSEC researchers have fabricated high efficiency and low cost unconventional cylindrical architecture solar devices for terrestrial applications by combining the solar cell design with a novel optical design. This approach allows multiple benefits including: decreasing the amount of active semiconducting materials to less than 5%, increasing the light absorption and conversion, improved performance with non-ideal (lower cost) materials, increased flexibility of the material choices and increase the overall efficiency. The concept is being demonstrated using organic materials (P3HT/PCBM) and a similar platform as used for high performance inorganic solar cells. The process uses inexpensive fabrication technologies which could define a new direction in the PV large-scale fabrication of this PV/optical device.

2011 Annual Report

FSEC researchers have fabricated high efficiency and low cost unconventional cylindrical architecture solar devices for terrestrial applications by combining the solar cell design with a novel optical design. This approach allows multiple benefits including: decreasing the amount of active semiconducting materials to less than 5%, increasing the light absorption and conversion, improved performance with non-ideal (lower cost) materials, increased flexibility of the material choices and increase the overall efficiency. The concept is being demonstrated using organic materials (P3HT/PCBM) and a similar platform as used for high performance inorganic solar cells. The process uses inexpensive fabrication technologies which could define a new direction in the PV large-scale fabrication of this PV/optical device.

The realization of a high efficiency/low cost solar hybrid device which is easily manufacturable is one of the defining problems of photovoltaics. Our innovation is to design an integrated optical/PV cell hybrid system allowing efficiency improvements while decreasing the costs, and hence expand the applications for solar energy. It utilizes a design approach which focuses first on performance, enabling the use of old or new photovoltaic materials. The flexibility of these architectures allows a wide portal to accommodate new breakthrough concepts because the device accepts light at wide angles from a large fraction of the sky and it is therefore able to capture most of the diffuse light, which makes up ~10% of the incident power in the solar spectrum.

Unconventional architectures: Photovoltaic/Optical Device

The PV/Optical glass rod cell consists of four layers deposited on a very thin glass or polymer fiber: a transparent anode shell, a positively charged/doped shell; a negatively charged/doped shell and a transparent cathode shell. [1] (fig.1) The light is incident on the fiber and cell and it is transmitted down the fiber and reflected multiple times from its interior surface, until passing through the active layers and absorbed or passed through the transparent electrodes, thus allowing for multiple passes through active layers of the incident or adjacent cells. Two metal layers separated by a dielectric material are used to collect the photo-generated charges. They constitute the device back side of the PV/optical hybrid device. The electrode shells of each cell are of different length, with the outer and shorter electrode shell connected to the upper metal layer, and the longer inner electrode shell passing through the dielectric layer and connecting to the lower metal layer. One of the metal layers is connected to the positively charged transport electrode and the second metal is connected to the negatively charged transport electron.

The PV device consists of many cylindrical cells imbedded into a polymeric matrix with nanoparticles which scatter the light back into the cells.[2] (fig.2)The key optical elements which enhance the light capture are: light trapped by the glass/polymer fiber, light transmitted through the transparent electrodes

(ITO and graphene), light absorbed and scattered by the nanoparticles imbedded into the polymeric matrix and, light reflected back into the device by the metallic substrate.

The key electrical elements which enhance the light conversion are: photo-excited electrons and holes traveling very short distances before being collected by the electrodes, which could decrease the electronic recombination caused by impurities, high anti-reflection, high surface energy which could increase EQE. [3]

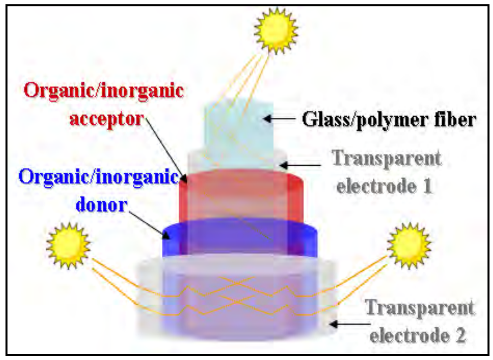

Figure 1: Rod and multifunction tube PV cells

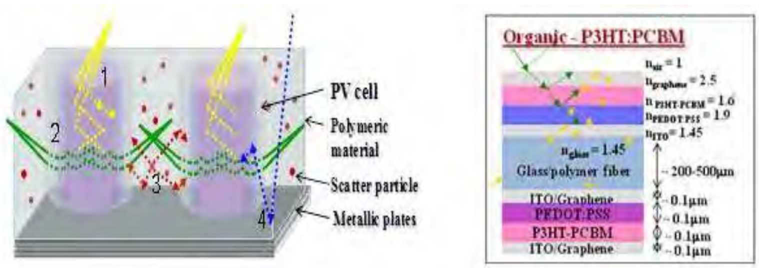

Figure 2. Schematic of the PV/optical device

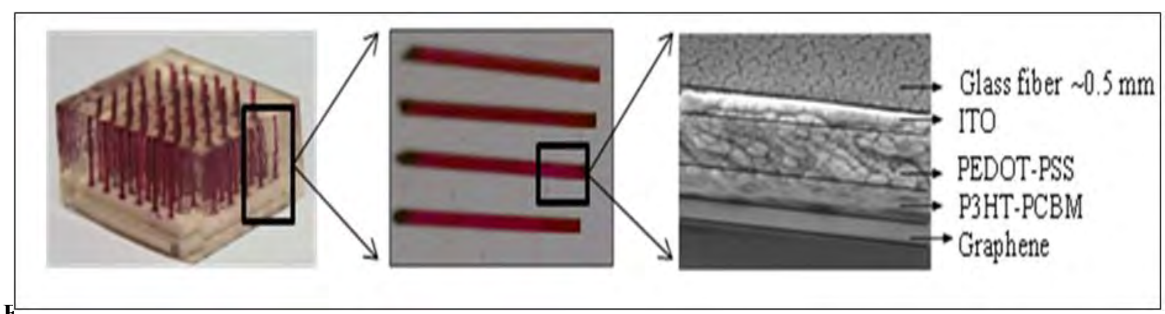

Figure 3: PV device

The first step in building the PV/Optical device was to fabricate and optimize the optical and electrical properties of the transparent graphene electrodes. They are the key elements in achieving high efficiency PV/Optical device.

Transparent electrodes fabrication and results:

GO can be readily obtained from exfoliation of graphite through oxidation. A stable 0.5 mg/mL GO aqueous dispersion (GO ethanol dispersion) was obtained by adding GO into DI water (ethanol) followed by 1 h (3 h) sonication. In order to achieve a highly uniform deposition, we employed a motor controlled two dimension airbrush spray coating system to deposit the GO dispersion onto a preheated glass substrate at about 70 ^{o}C. The moving speed of air brush is set as 19 mm/s. Spray rate is about 3-10 µL/s, controlled by the pressure of N_2. The GO coatings in different thickness were achieved by controlling the runs of spray. The as prepared GO coatings were covered by quartz glass, then, reduced by 6 h UV radiation under a 40 W UV light and followed by annealing under Ar atmosphere at 400 ^{o}C for 30 min.

Optical properties of sprayed GO coatings and RGO coatings were studied. The GO coatings showed very high light transmittance. Even GO coating sample with 8 runs spray still gave a transmittance around 80% (Fig.5) at 550 nm. After reduction, the transmittance of graphene could show a decrease. For example, a 92% transmittance was observed on the 4 runs spray coating GO sample. After UV reduction, the transmittance dropped to 65%. Then, a slight decrease was also observed after the thermal reduction, resulting into a 63% transmittance. We also noticed there is a slight increase of the transmittance at UV band (below 360 nm), which is very interesting. It might be explained that the electronic conjugation within graphene sheets was further restored by the thermal reduction, which caused a redshift of the absorption peak and a change of the intensity at UV band [5]. Drop coating and spin coating methods were attempted in the deposition of GO coatings. However, these experiments all resulted in uneven GO platelets as water (H2O) or ethanol (EtOH) evaporated and GO concentrated. Only spray coating on hot substrate generate a uniform coating that show almost the same transmittance spectra at different position of one GO Coating. It might be explained that the small droplets and immediate evaporation prevented the GO platelets from aggregating.

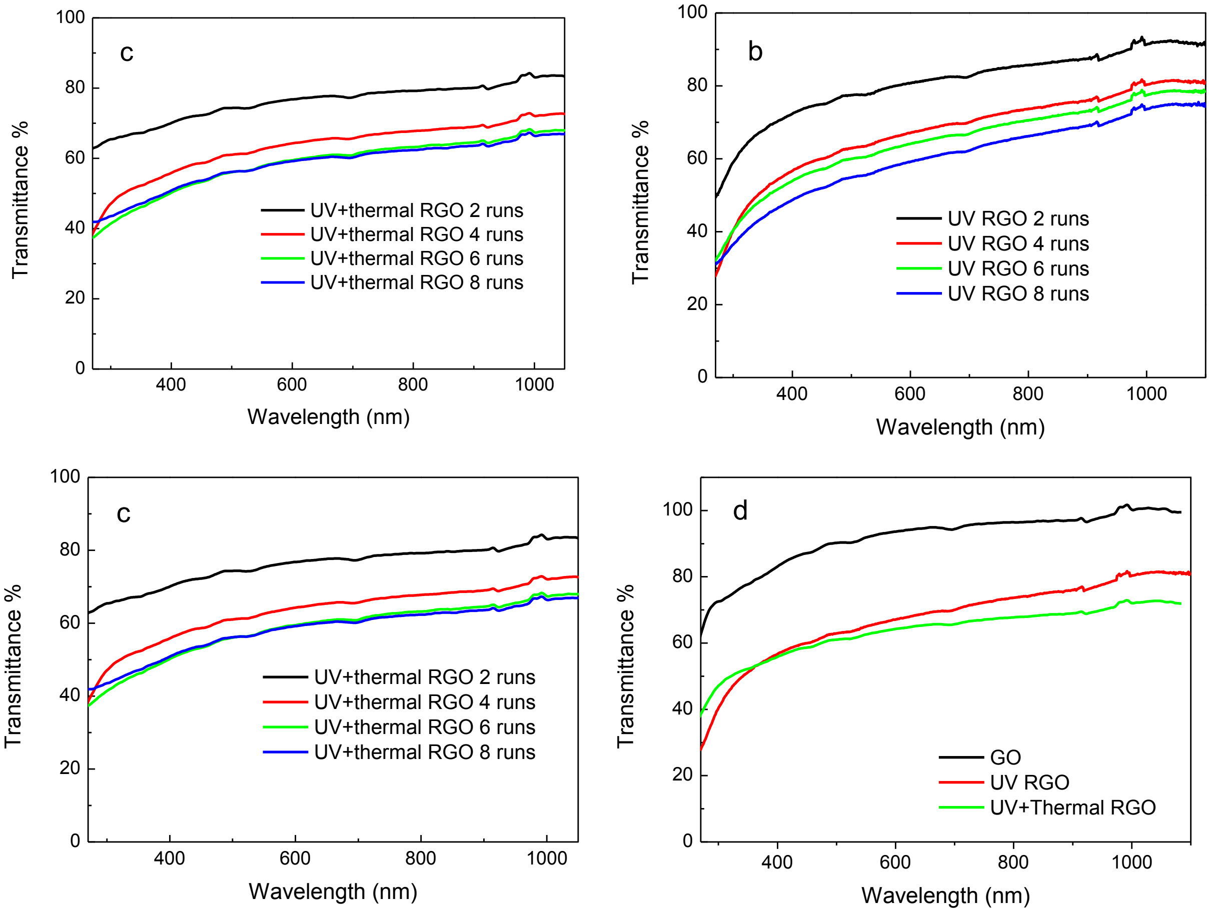

Fig. 5: Transmission spectra of GO coatings with 2, 4, 6 and 8 run sprayed with GO/H_2O. (a, GO coatings. b, UV treated RGO coatings. c, UV+thermal treated RGO coatings). d, Transmission of 6 runs GO coating before and after treated.

Raman spectra of the GO film before and after the reduction process are shown in Fig. 6. Of particular interest is the disorder-induced characteristic Raman 'D' peak at around 1340 cm−1 [6] and a broad G-band at 1580 cm-1, the latter corresponding to the first-order scattering of the E2g mode [7,8]. Another peak at 2940 cm−1, close to the second-order features such as 'D + D'' [9] or 'D + G'' [10], is also observed. The 2D peak is too weak in intensity to be observed. The prominent D peak is from the structural imperfections created by the attachment of hydroxyl and epoxide groups on the carbon basal plane. After UV and heat treatment, the magnitude of D band peak dropped, and the ID/IG ratio decreased from 0.755 to 0.708, which indicates a reduction of the GO film[11]. The behavior of ID+D'/IG (dropping from 0.237 to 0.192) also shows a matching result.

Fig. 6. Raman spectra of D and G band, with inset showing the D+D' band for 6 run spray coating GO and RGO films.

Fig. 7 shows the SEM images of RGO films sprayed with GO/H2O (Fig 7a-d) and GO/EtOH dispersions (Fig 7e-h). The SEM image of hydrazine vapor treated RGO film (Fig.7a) indicates a homogeneous morphology of graphene coatings. Graphene exhibits typical wrinkled structure with corrugation and scrolling which is intrinsic to graphene, whick may be important for preventing aggregation of graphene due to van der Waals forces during drying and maintaining high surface area[12,13]. On the image of 200 oC thermal treated RGO in standard N2 atmosphere (Fig.7b), micro aggregations were observed forming the shape of small water droplets. It suggests the GO might aggregate slightly when the small water droplet dries. Some graphene pieces were also found on the RGO film. When heating to 400 oC under standard N2, the RGO film was burned by the small amount of oxygen in the standard N2 (Fig.7c). Fig.3d shows the RGO film treated by UV and 400 oC heating under pure Ar (99.999%). Structures like water droplets were still observed, and small pieces of graphene were also found on the RGO film.

Structures of droplets were not found in fig 7e. The RGO film looks very smooth and clean with only a small amount of isolated graphene pieces on it. Since ethanol evaporates faster than water, we employed bigger ethanol droplets to form a very thin ethanol film during the spray process. At about 70 oC, the ethanol film dried very fast on the glass substrate and the GO did not concentrate, generating a very homogenous GO film. However, it is difficult to dry a thin water film immediately, even at a higher temperature. A few droplet structures were found on the film sprayed with smaller droplets (fig 7f). Also, more isolated graphene pieces were observed. The RGO samples with thinner films (fig 7g, h) showed uneven and discontinuous RGO film. Single layer graphene films were observed here.

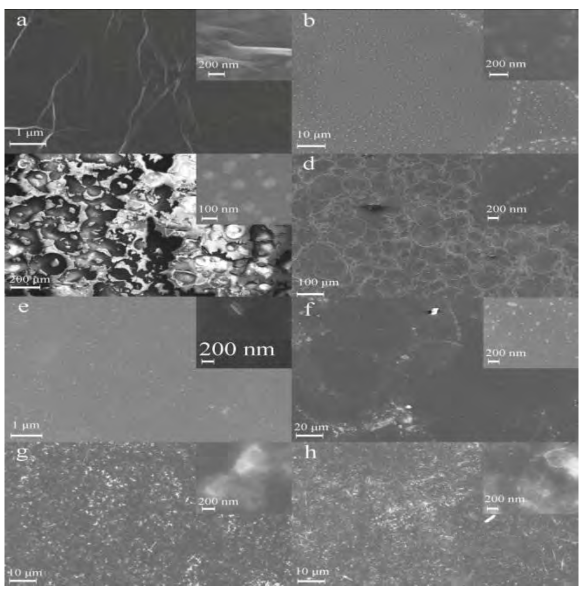

Fig. 7: TEM images of RGO coatings treated by a, Hydrazin. b, 200 ^oC, N_2. c, 400 ^oC, N_2. d-h, 400 ^oC, Ar. (Spray setting: a-d, sprayed in 5 μL/s for 8 runs with GO/H_2O dispersion. e, sprayed in 10 μL/s for 5 runs with GO/EtOH dispersion. f, sprayed in 7 μL/s for 7 runs with GO/EtOH dispersion. g, sprayed in 5 μL/s for 5 runs with GO/EtOH dispersion. f, sprayed in 3.5 μL/s for 7 runs with GO/EtOH dispersion.)

AFM images were studied to further discover the morphology and measure the thickness of the RGO films (Fig. 8). The image shows RGO film is formed by several layers of graphene and the film is very smooth even in a large scale (5 μm). By scratching the RGO film, we also measured the thickness as 6 nm.

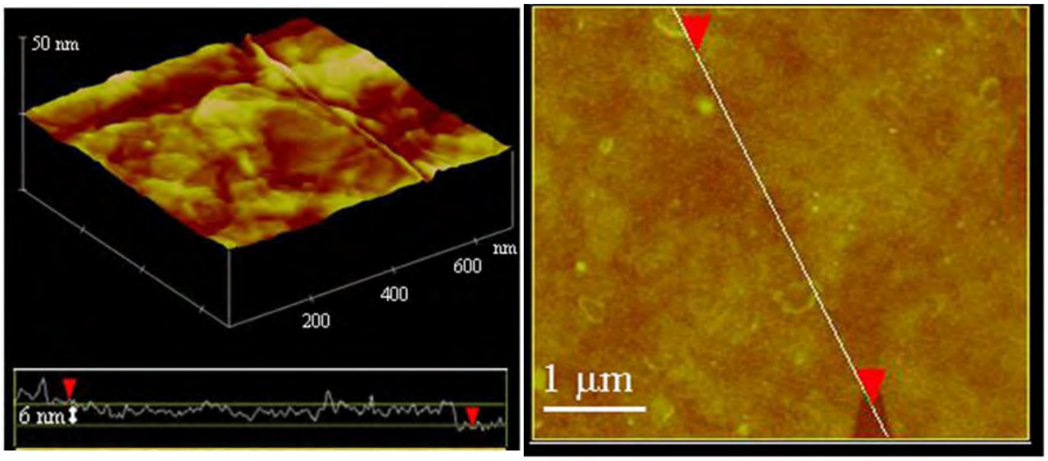

Fig 8: AFM images of RGO films sprayed in 10 µL/s for 5 runs with GO/EtOH dispersion and treated by UV and thermal annealing at 400 °C Ar.

In summary, we report a method to deposit uniform and controllable GO coatings by spray coating. Homogeneous RGO coatings were achieved by combined reduction with UV and annealing under Ar atmosphere. The graphene coatings show promising applications on transparent and conductive electrodes. We will employ graphene coatings to fabricate the enhanced light harvesting solar cells in further work.

Donor-acceptor fabrication (PEDOT-PSS, P3HT/PCBM):
For standard devices a layer of 0.45 µm filtered PEDOT: PSS was sprayed in a temperature controlled environment onto ITO coated glass fibers which were then annealed at a temperature of 125 °C for 1 minute. A layer of 0.45 µm filtered 1:0.8 P3HT: PCBM was then sprayed forming the active layer of the devices and following that the devices were solvent annealed for 5 minutes. Studies of the thickness and thermal annealing were performed in order to optimize the power conversion efficiency.[4]

References:
[1]. Yuan Li, Eric D. Peterson, Huihui Huang, Mingjun Wang, Dan Xue, Wanyi Nie, Wei Zhou, and David L. Carroll, *Tube-based geometries for organic photovoltaics*, Appl. Phys. Lett. 96, 243505 (2010);

[2]. Joseph Lik Hang Chau, Ruei-Tang Chen, Gan-Lin Hwang, Ping-Yuan Tsai, and Chien-Chu Lin, *Transparent solar cell window module,* Solar Energy Materials and Solar Cells, Volume 94, Issue 3, March 2010, Pages 588-591

[3]. Hsin-Cheng Lee, Shich-Chuan Wu, Tien-Chung Yang and Ta-Jen Yen, *Efficiently Harvesting Sun Light for Silicon Solar Cells through Advanced Optical Couplers and A Radial p-n Junction Structure,* Energies 2010, *3*, 784-802;

[4]. Youngkyoo Kim, Amy M. Ballantyneb, Jenny Nelsonb and Donal D.C. Bradleyb, *Effects of thickness and thermal annealing of the PEDOT:PSS layer on the performance of polymer solar cells,* Organic Electronics, Volume 10, Issue 1, February 2009, Pages 205-209

[5] D. Li, M. B. Müller, S. Gilje, R. B. Kaner, G. G. Wallace. Nature Nanotechnology 3, 101-105 (2008)

[6] A. C. Ferrari. Solid State Commun. 143, 47-57 (2007)

[7] M. Ramm, M. Ata, T. Gross, W. Unger. Appl Phys A: Mater 70, 387–90 (2000).

[8] D. Yang, A. Velamakanni, G. Bozoklu, S. Park, M. Stoller, R. D. Piner, S.Stankovich, I. Jung, D. A. Field, C.A. Ventrice Jr., R. S. Ruoff, Carbon. 47, 145-152 (2009)
[9] T. Gokus, R. R. Nair, A. Bonetti, M. Boehmler, A. Lombardo, K. S. Novoselov, A. K. Geim, A. C. Ferrari, A. Hartschuh, ACS NANO 3, 3963-3968 (2009).
[10] J.Campos-Delgado, J. M. Romo-Herrera, X. Jia, D. A. Cullen, H. Muramatsu, Y. A. Kim, et al Nano Lett. 8, 2773-2778 (2008)
[11] I. Childres, L. A Jauregui, J. Tian, Y. P Chen. New J. Phys. 13, 025008-025020 (2011)
[12] M.J. McAllister, J.L. LiO, D.H. Adamson, H.C. Schniepp, A.A. Abdala, J. Liu, M. Herrera-Alonso, D.L. Milius, R. CarO, R.K. Prud'homme, I.A. Aksay, Chem of Mater. 19, 4396-4944 (2007)
[13] R. Kou, Y.Y. Shao, D.H. Wang, M.H. Engelhard, J.H. Kwak, J. Wang, V.V. Viswanathan, C.M. Wang, Y.H. Lin, Y. Wang, I.A. Aksay, J. Liu, Electrochemistry Communications 11, 954-957 (2009)

Florida Energy Systems Consortium

University of Central Florida
Solar Systems Testing Facility

PIs: James Roland, David Block

Description: Over the past five years, the Florida Solar Energy Center (FSEC) has received a significant increase in demand for solar thermal and PV testing and certification. This occurrence has resulted in requiring the Center to correspondingly amplify its capabilities to respond to the increased demand. Thus, the objective of this task was to construct a solar thermal and PV systems testing facility. This facility was built by adding walls, windows, doors and air conditioning to an existing roof only facility at the FSEC site. This new facility provides laboratory space for testing of solar water heating components and systems and PV modules and inverters. At this time, the facility is completed and this is the final report for the project.

Budget: $600,609
Universities: UCF/FSEC

Executive Summary

The building renovation has been completed and the new facility is now called the Solar Systems Testing Facility (Bldg. #1940). The following photographs show the facility before any renovations were begun (Figure 1) and the exterior and interior views after renovation (Figures 2 to 4). The action to enclose the existing roof facility was taken following a study which determined this action was the most cost effective means of adding valuable indoor laboratory space.

Figure 1: Ground Level Front View

Figure 2: Exterior View After Completion

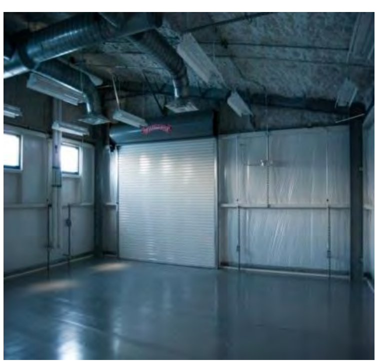

Figures 3 and 4: Interior Views – Ready for Laboratory Installation

Within the new facility, two laboratories plus technician offices have been developed and construction is complete. Both of the laboratory development projects are part of the FESC program and are reported in greater detail under the following two projects:

1. Enhanced and Expanded Solar Thermal Testing Capabilities, PI: John DelMar, Joe Walters
2. Enhanced and Expanded PV Systems Testing Capabilities at FSEC, PI: Stephen Barkaszi

2011 Annual Report

Results
At this time, the facility is completed and this is the final report for the project. For information purposes, in 2005, the cost of the original 4,500 ft^2 roof only facility was $165,947 or $36.88 per sq. ft. FESC funds were used in 2009 to enclose and air condition giving a building cost of $437,316 or $116.62 per sq. ft. The entire roof structure building was not enclosed, only 3,750 ft^2. These values give a total building cost of $603,263 or $153.50 per sq. ft.

Background
The Florida Solar Energy Center (FSEC) is one of the nation's leading testing and certification organizations for solar products and equipment. The center's expertise is based on over 40 years' experience conducting accredited solar energy testing and certification programs. FSEC believes that independent, third-party testing and certification has extensive value in the marketplace, especially for products that are not widely "proven" with consumers such as solar water heating systems and solar electrical (photovoltaic) systems. Independent, third-party certification provides not only protection for consumers, but also much needed consumer confidence. Even more important, third-party certification provides protection to reputable manufacturers, ensuring that lower quality products, often from foreign markets, do not compete head-to-head with Florida and U.S. products unless they meet the same standards.

Due to the resurgence of the solar industry, FSEC has received a significant increase in demand for solar collector and solar system testing and certification. This occurrence has resulted in requiring the Center to correspondingly amplify its capabilities to respond to the increased demand.

Thus, the objective of this project was to add walls, windows, doors and air conditioning to an existing FSEC roof only facility for the purpose of increasing indoor and air-conditioned laboratory space and to allow for conducting tests on solar water heating systems and PV modules and inverters.

Existing Facility
In 2005, FSEC constructed a slab and roof only facility. The purpose of this facility was to allow for PV module and inverter testing and for hydrogen research. Due to the increase in testing and certification requirements, the need for conditioned laboratory space became a critical requirement. Thus, the most cost-effective program that could be done to add laboratory space was to design and construct an enclosure for the existing roof facility.

I. Solar Thermal Testing

FSEC's solar thermal systems laboratory has been moved from its previous location to the new lab and the required system mounting racks and storage tanks have been redesigned and are now in place for testing. The new system lab now operates more efficiently with regard to testing time and reporting of test results. The photo in Figure 5 shows the tank setup and storage tanks.

Figure 5: Solar Thermal Testing Lab

II. PV Systems Testing

The PV Systems Testing part of the facility conducts testing on PV inverters and has a new long pulse simulator manufactured by Spire Corporation. The photo in Figure 6 shows the Spire pulse simulator and Figure 7 shows the inverters testing.

Figure 6: PV Simulator

Figure 7: PV Inverter Testing

Industry Support:

This task is supported by testing fees received from the solar thermal and PV manufacturers who must have certification to sell their products in Florida and to qualify those products for various other state and federal incentives and rebates.

This project has been completed.